

Mechanical, thermal and morphological studies of microfibrillated jute/PLA biocomposites

G M Arifuzzaman Khan¹, M Abdullah-Al-Mamun¹, M Ahsanul Haque¹, Md Shafiqur Rahman¹, Hamid Shaikh², Arfat Anis², Saeed M Al-Zahrani² & M Shamsul Alam^{1,a}

¹Polymer Research Laboratory, Department of Applied Chemistry & Chemical Engineering, Islamic University, Kushtia, Bangladesh

²Chemical Engineering Department, King Saud University, P. O. Box 800, Riyadh 11421, Saudi Arabia

Received 9 February 2015; revised received and accepted 4 September 2015

In the present study, biocomposites based on microfibrillated jute (MFJ) fibre and polylactic acid (PLA) have been prepared by solvent-assisted compression moulding techniques. The MFJ is obtained by a sequence of alkali, chlorite and acid treatments of jute fibre. The biocomposites are fabricated by loading of 10, 20 and 30 wt% of MFJ fibre into the PLA matrix. The effect of MFJ fibre loading on the mechanical, thermal, and morphological properties of the composites is also studied. Among these composites, it is observed that 10 wt% fibre-filled biocomposite shows improved tensile strength and tensile modulus compared to virgin PLA film. Similarly, storage modulus and loss modulus are also found improved for the composites. These composites exhibit higher water absorption capacity and lower thermal stability than virgin PLA. The fibre-matrix adhesion is evaluated by scanning electron microscopy. The results are attributed to the improved interfacial adhesion between MFJ and PLA matrix for 10 wt% fibre-filled biocomposites.

Keywords: Biocomposites, Mechanical properties, Microfibrillated jute, Morphological properties, Polylactic acid, Thermal properties

1 Introduction

The uses of petroleum based packaging material in domestic and industrial purposes are increasing continuously. As a result, solid waste disposal or management is becoming a great challenge in urban and rural areas. Various processing methods to eliminate plastics wastes such as biodegradation, recycling, incineration are considered as attractive solutions. Among them, uses of fully biodegradable polymer have a well-grounded role in minimizing this problems^{1,2}. Therefore, growing interest in use of biodegradable commodity plastic is increasing in the field of ecology to reduce environmental pollution.

In the family of biodegradable polymer, polylactic acid (PLA) appears to be one of the most attractive materials. It is widely used in biomedical applications, especially for artificial implants and bone fixation because of its biocompatibility, bioabsorbability and good mechanical properties^{3,4}. PLA is a strong competitor in the plastic market having similar properties to that of polyethylene terephthalate (PET), which makes it suitable for the food-packaging

sectors. However, high production cost and low impact failure restricted its use in commercial scale. In order to secure its demand in the global market, it is desirable to enhance its physical as well as chemical properties such as thermal stability, good mechanical strength and ease of processability. The development of PLA based biocomposites with cheap and renewable reinforcement fillers are one way to achieve these properties.

With the aim to developing sustainable “green composites”, researchers have used various plant fibres as reinforcement fillers for PLA⁵. The plant fibres are mostly composed of cellulose, hemicellulose, lignin, pectin, wax, etc. The morphology and mode of combination of these constituents is quite complicated, and due to complex topography plant fibres composites often show anisotropic nature⁶. A sequence of various chemical treatments, such as acid hydrolysis, alkali, and NaClO₂ bleaching can extract the fibres cellulose from plant biomass. The resultant fibre may contain 90-95% of the α -cellulose. Owing to its high molecular weight and chemically stable nature, the α -cellulose is recently investigated as green fillers as biocomposites fabrication by various compounding methods^{7,8}.

^aCorresponding author.
E-mail: dr.alamiu@yahoo.com

The interfacial interactions between microfibrillated cellulose (MFC) fibres and polymer matrix play a crucial role in the local stress transfer, which determines the overall mechanical properties of the composites⁹⁻¹¹. A poor interfacial adhesion between the MFC and the polymer matrix will introduce artificial defects, which consequently results in a deleterious effect on the mechanical properties of the composites. Introducing good linkages between the MFC and the PLA for better adhesion is still challenging for specific composite fabrication. However, appropriate chemical modifications of the MFC surface by chemical functional groups could improve the uniform dispersion ability and compatibility with the matrix by formation of chemical bonds.

Various modifiers have been used to improve compatibility between cellulose fibre and PLA such as triacetin¹², benzoyl peroxide¹³, maleic anhydride¹⁴, etc. The C=C groups of maleic anhydride attached on cellulose fibres can undergo chemical reaction with the PLA matrix which causes the better adhesion between the filler and the matrix. However, the surface modification of MFC with a modifier is not always provided high strength and modulus of composites. The proper distribution of filler in the matrix, void content also affects the overall properties of the composites.

In this study, attempts have been made to prepare the microfibrillated jute fibres from jute fibres. These microfibrillated jute fibres are surface functionalized with maleic anhydride to improve adhesion property. The fabrications of composites based on this fibre with PLA matrix have been accomplished by solvent-assisted compression moulding method. The mechanical, thermal, morphological properties and microscopic changes of these biocomposites are investigated in detail.

2 Materials and Methods

2.1 Materials

The jute fibre was collected from local market of Jhenidah district, Bangladesh and 60 cm from the middle portion of the stem was taken. PLA ($M_w=1,10,000 \text{ gmol}^{-1}$, $M_p=160-170^\circ\text{C}$) was synthesized from L-lactic acid (Purac, 90%, Netherland) by direct polycondensation method¹⁵. Maleic anhydride (MA), tetrahydrofuran (THF), sodium carbonate, acetic acid, sodium acetate, sodium chlorite, sodium metabisulphite and chloroform were purchased from Merck, Germany, and used as a received.

2.2 Preparation of MFJ Sample

The untreated jute fibres (20 g) were immersed in 1L of NaOH solution (17 w/v%) for 3h at room temperature. Then the fibres were washed with distilled water until it is free from alkali. After washing, it was kept in oven for air drying at 80°C for 6h (ref. 16). The alkali-treated jute fibre was bleached using NaClO₂ (7 g/L) solution buffered at pH 4 and at 90-95°C for 90 min, maintaining the fibre-to-liquor ratio at 1:50. After completion of the bleaching reaction, the fibre was treated with 0.2% sodium metabisulphite solution for 15 min to reduce chlorite action, and then washed thoroughly with distilled water¹⁷. The resultant bleached fibre looks like cotton and it contains 92-95.5% α -cellulose as measured by TAPPI method¹⁸.

The bleached fibre was taken in 3N H₂SO₄ solution at room temperature, maintaining the fibre-to-liquor ratio at 1:50. The hydrolysis reaction was carried out by continuous stirring with magnetic stirrer for 3h. This reaction was carried out to hydrolyze the amorphous region of the cellulose, which result in cellulose fibre with high crystallinity. The obtained microfibrillated jute (MFJ) fibres then dispersed in tetrahydrofuran (THF) solution by using an ultrasonic bath at the duration of 3h. The fine powder of MFJ fibres was obtained after removing THF solvent.

The surface functionalization of fibres was carried out in maleic anhydride solution. A maleic anhydride (MA) was dissolved in dimethylformamide (DMF) at ratio of 1:20. The MFJ fibres were added to the MA solution (MFJ: MA=20:1) and heated at 60°C for 3h with constant stirring. The treated fibres were then filtered and rinsed with acetone to remove the unreacted MA. The fibres were washed by refluxing with acetone for 5 times and dried in an oven at 60°C for 3h.

2.3 Preparation of MFJ-PLA Biocomposite

A known amount of PLA was dissolved in a minimal amount of chloroform. The MFJ fibre with fixed amount was also dispersed in chloroform separately. These dispersions were mixed at the appropriate weight ratio and stirred at ambient conditions. Then the blend was taken in female part of stainless steel close mould and placed in an oven to evaporate chloroform. The mould was retrieved from the oven before complete hardening. The mould was capped by male part and uniform film was pressed by using hot press moulding machine. This mould was constructed with capillary ventilations to remove unwanted gases from blend. The mould was kept for

30 min at 80°C by applying 50 KN pressure. Afterward, it was cooled by tap water and a mould releasing spray (BONEY-Mould release silicon spray, manufacture-London chemicals Ind. England) was used to easy opening of the mould.

2.4 Measurements

The tensile tests were carried out according to ASTM D882 (E) using Universal Testing Machine (Hounsfield UTM 10KN). The clamping length for each specimen on each jaw was 15 mm and no extensometer was used for tensile tests. The tests were performed at a crosshead speed of 5 mm/min. The tensile modulus and elongation were determined from stress-strain curve by QMAT tensile test software.

Temperature dependent dynamic viscoelastic properties of the composites was measured by a thermo mechanical analyzer (EXSTAR TMA/SS6300) with a chuck distance of 20 mm, preload of 5g, frequency of 1 Hz and heating rate of 1.5°C/min.

The extent of water absorption of neat PLA and biocomposites were determined as per ASTM D570. The dimension of composite test specimens was 7.5×2.5×0.3 cm³. The specimens (dry weight W_1) were kept in water at 50°C for 24h and final weights (W_2) were taken. A percentage of water absorption was calculated by using following equation:

$$\text{Water absorption (\%)} = \frac{(W_2 - W_1) \times 100}{W_1}$$

The thermogravimetric analysis of samples was conducted by thermal gravimetric analyzer (TG/DTA 6300, Seiko Instrument Inc., Japan). About 15-20 mg of each sample was taken for analysis. The samples were heated up steadily at a rate of 20°C/min from 25-600°C under a continuous flow of nitrogen at the rate of 50 mL/min. The analysis was carried out twice for each specimen.

The surface morphology of biocomposite samples was observed by scanning electron microscope (JEOL 6400) with accelerating voltage of 10 kV. The surface was coated with 3 nm thick gold before analysis.

Fourier-Transform Infrared Spectroscopy (FTIR) analysis of samples was measured on Shimadzu IR-470 spectrophotometer (Shimadzu, Kyoto, Japan). A small amount of the samples was mixed in KBr to make a transparent pellet. The FTIR spectrum between 450 cm⁻¹ and 4000 cm⁻¹ with accumulation of 20 scan and resolution of 4 cm⁻¹ was recorded.

Wide Angle X-Ray Diffraction (WAXRD) pattern was obtained with a Bruker D8 Advance wide angle X-ray diffractometer using Cu K α radiation ($\lambda=0.154$ nm), voltage of 50 KV and current of 40 mA with 2 θ range from 5°- 40°, increased in step of 2°/min.

3 Results and Discussion

3.1 Tensile Properties

The tensile behavior of neat PLA and its biocomposites as a function of fibre loading is given in Table 1. Generally, the fillers play an important role in determining the tensile properties of cellulose filled thermoplastics as reported in the literature⁸. It is observed that the tensile strength of MFJ/PLA composite is increased up to 10 wt% fibre loading. This property appears to be decreased with the further increase in fibre contents. This could be due to the change from ductile to brittle fracture behavior with increasing fibre content. Also, the decrease in tensile strength of the composites might imply non-uniform stress transfer in the matrix due to fibre agglomeration. It is observed that at 10 wt% and 20 wt% fibre loading, the tensile strength increased by 40% and 25.3% respectively as compared to neat PLA, while in a case of 30 wt% fibre loading, the tensile strength is decreased by 8.2% compared to neat PLA. At higher percentage of fibre loading, the tensile strength is decreased due to weak interfacial adhesion. A similar trend in decreasing tensile strength with increasing filler content has also been reported¹⁹.

The tensile modulus of neat PLA and its composites are obtained from the tangents of stress-strain curves (Fig. 1). Similar to the tensile strength, the tensile modulus is also improved significantly at 10 wt% and 20 wt% fibre loading. The tensile modulus of these biocomposites increased by 28.8% and 13.2% respectively as compared to neat PLA. The improvement in tensile modulus can be attributed to the better stress propagation between the fillers and the matrix. The increase of tensile modulus with the addition of MFJ fibre is in good agreement with other cellulose filled polymer composites²⁰. The decrease in tensile modulus value at higher percentage of fibre

Table 1 — Mechanical properties of MFJ/PLA biocomposites

MFJ/PLA composite	Tensile strength MPa	Tensile modulus MPa	Strain %
0 wt% MFJ fibre	34.0±5.2	365±11	3.40±0.42
10 wt% MFJ fibre	47.6±3.7	470±90	4.78±0.57
20 wt% MFJ fibre	42.4±3.3	413±12	3.76±0.80
30 wt% MFJ fibre	31.0±7.8	298±16	2.92±0.84

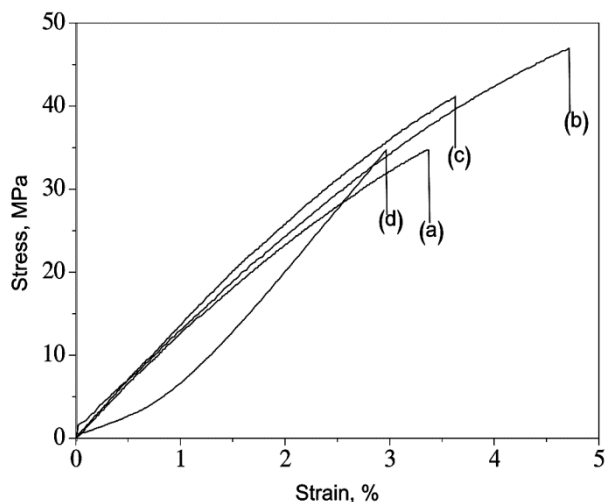


Fig. 1 — Tensile stress-strain curves of MFJ/PLA composites (a) neat PLA, (b) 10 wt% MFJ, (c) 20 wt% MFJ, and (d) 30 wt% MFJ fibres

loading is mainly due to the fibre agglomerations, which obstructs stress propagation. Therefore, well-dispersed fillers prevent the obstruction of stress propagation and restrict the molecular mobility. Similar trends for the elongation percentage are observed. It is found that at 10 wt% and 20 wt% fibre loading, elongation percentage of biocomposites is increased 40.5% and 10.6% respectively, which is higher than neat PLA. This may be due to the reduction in brittleness of PLA in addition of the MFJ fibre. This behavior of biocomposites is also reported in other cellulosic reinforced PLA composites²¹. Subsequently, the elongation at maximum stress is decreased with 30 wt% fibre loading. The elongation is found to be 14.1% lesser than neat PLA. The higher fibre loading of composite have more ductility that may cause early rupture of composites.

3.2 Dynamic Mechanical Property

The storage modulus is a useful parameter in assessing the molecular basis of the mechanical properties of material. It is very sensitive to structural changes such as fibre–matrix interfacial bonding, and is closely related to the load-bearing capacity of composites materials²². Fig. 2 shows the storage modulus of 10, 20, and 30 wt% fibre filled PLA biocomposite as a function of temperature. It appears that the modulus decreases with the increase in temperature. The reduction in modulus may be associated with softening of the matrix at higher temperature²³. There is a notable increase in the storage modulus of PLA matrix with the incorporation

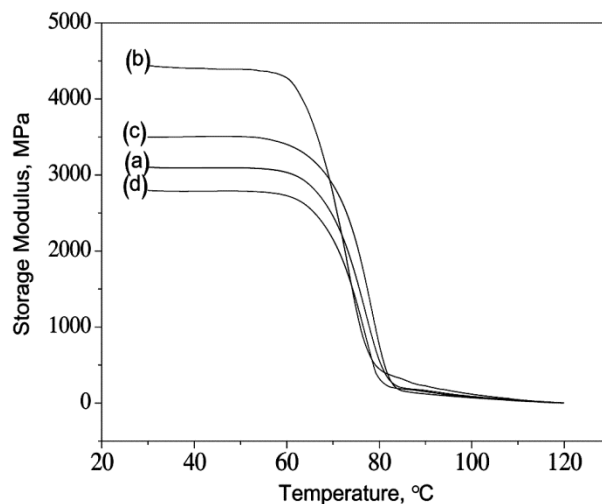


Fig. 2 — Storage modulus of MFJ/PLA composites (a) neat PLA, (b) 10 wt% MFJ, (c) 20 wt% MFJ, and (d) 30 wt% MFJ fibres

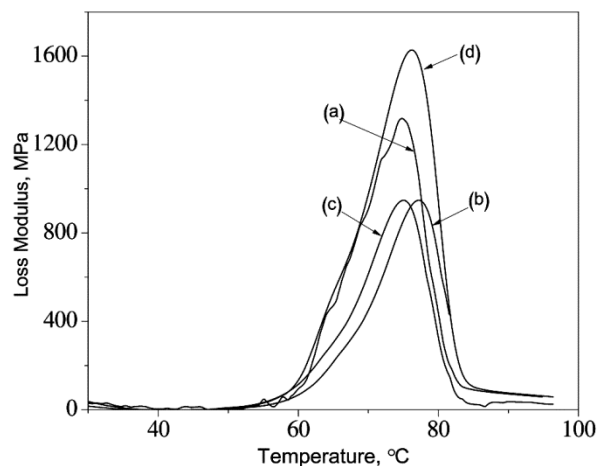


Fig. 3 — Loss modulus curves of MFJ/PLA composites (a) neat PLA, (b) 10 wt% MFJ, (c) 20 wt% MFJ, and (d) 30 wt% MFJ fibres

of 10 wt% fibres as compared to other concentration. This is probably because of the increase in the stiffness of the matrix with reinforcing effect imparted by the MFJ fibre, which allowed a greater degree of stress transfer at the interface. The high modulus could be because of intermolecular bonds and rigid skeletal conformation of cellulose molecule²⁴. However, the storage modulus is decreased after 10 wt% fibre content in biocomposite. This could suggest that the high quantity of fibre is not well dispersed in PLA matrix.

Figure 3 shows the loss modulus of neat PLA and 10, 20 & 30 wt% fibre-filled PLA composites. It is known that the loss modulus is proportional to the amount of energy that has been dissipated as heat by the material. The loss modulus peak is attributed to

the mobility of the resin molecules. This peak occurs at the glass transition temperature (T_g) of the material²⁵. As shown in Fig. 3, the loss modulus decreases with the presence of 10 wt% and 20 wt% of fibre loading. According to Liu *et al.*²⁶, one possible explanation of this phenomenon is that neat PLA shows a sharp and intense peak because there is no restriction to the chain motion. The MFJ fibres can hinder the chain mobility, which results in the reduction of sharpness and height of the loss modulus peak. Fay *et al.*²⁷ also reported a reduction in the loss modulus peak due to the immobilization of polymer matrix in the presence of the filler. The reduction in loss modulus also denotes an improvement in the hysteresis of the system and a decrease in the internal friction. However, increase of loss modulus is found for higher fibre loading which indicates improper distribution of fibres in PLA matrix.

3.3 Water Absorption Properties

The water absorption properties of biocomposites play a crucial role for their practical applications. The water absorption study is carried out for 24 h in cold water for neat PLA and its MFJ/PLA biocomposites. The results are given in Table 2. It is found that the water absorption by neat PLA is 2.11% and it increases to 3.06, 4.88 and 6.50% for 10, 20 and 30 wt% fibre loaded composite respectively. The water absorption of MFJ fibre filled biocomposites is mainly because of the presence of hydrophilic cellulosic fillers. The water absorption increases proportionally with increasing MFJ fibre content. It is known that the factors like porosity content and filler–matrix adhesion are responsible for the moisture absorption behavior of the cellulose based biocomposites. Moreover, due to hydrophilic nature of the MFJ, the composites can absorb high amount of water, as the water tends to get retained in the inter fibrillar space of the cellulosic structure and micro voids present in the biocomposites.

3.4 Thermal Properties

The thermal stability of MFJ, neat PLA and MFJ/PLA biocomposites prepared with various amount of fibre loading has been studied by thermogravimetric analysis in nitrogen atmosphere. Fig. 4 shows the weight percentage change as a function of temperature. It appears that the degradation of neat PLA starts at a higher

temperature than that of MFJ and MFJ/PLA biocomposites. The decomposition of pure PLA is started at $\sim 310^\circ\text{C}$ and completed at $\sim 420^\circ\text{C}$. The MFJ fibre appears to be unstable when subjected to high temperature. This behavior is also reported in the literature²⁸. The onset temperature of MFJ is found 160°C and major weight ($\sim 47\%$) is lost before 220°C . However, the onset temperature and main degradation temperature increase proportionally with PLA contents. The initial weight loss of biocomposites at 120°C is due to removal of moisture. The decomposition temperature of 10 wt% and 20 wt% fibre filled biocomposites is found to be much higher than that of 30 wt% fibre reinforced biocomposites. The main degradation of 30wt% fibre filled biocomposite is started at 180°C and rapid weight loss continued upto 310°C for decomposition. These results demonstrate that 10 wt% and 20 wt% MFJ fibre reinforced biocomposites are well bonded with the PLA matrix. It is observed that 10 wt% of MFJ fibre filled biocomposite shows higher thermal stability than other biocomposites. The residual mass of MFJ fibre, neat PLA and MFJ/PLA biocomposites at 600°C are shown in Fig. 4. As expected, it is

Table 2 — Water absorption property of MFJ/PLA biocomposites

MFJ/PLA composite	Water absorption, % (at 30°C)
0 wt% MFJ fibre	2.11
10 wt% MFJ fibre	3.06
20 wt% MFJ fibre	4.88
30 wt% MFJ fibre	6.50

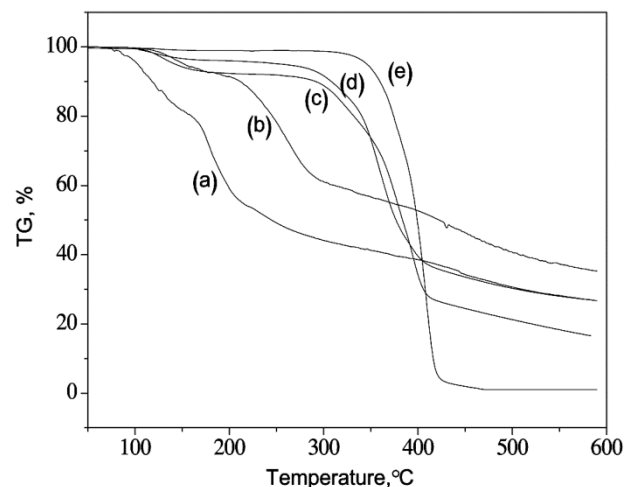


Fig. 4 — TG curves of MFJ/PLA composites (a) MFJ, (b) 30 wt% MFJ, (c) 20 wt% (d) 10 wt% MFJ fibres, and (e) neat PLA

observed that very minor char is remained for neat PLA, whereas the residual char content increases proportionally with MFJ fibre contents.

The derivative thermal gravimetry (DTG) is further studied to know the rate of weight loss with temperature and is shown in Fig. 5. The neat PLA shows only single peak at 388°C due to main degradation. On the other hand, the multiple peaks

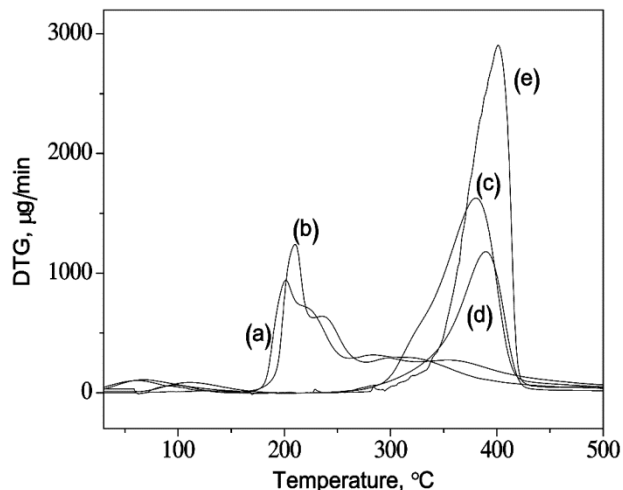


Fig. 5 — DTG curves of MFJ/PLA composites (a) MFJ, (b) 30 wt% MFJ, (c) 20 wt% MFJ (d) 10wt% MFJ fibres, and (e) neat PLA

appear at DTG curves for MFJ filled PLA composites. The initial peak at 120°C is due to moisture contents. The presence of multiple degradation peaks of MFJ fibre indicates the different molecular size of cellulose present in MFJ fibre, and their degradation takes place at different temperature. A single decomposition peak of 10 wt% and 20 wt% fibre-filled composites indicates the better adhesion between the fillers and the matrix.

3.5 Morphology

SEM images of tensile fracture surface of neat PLA and MFJ/PLA composites are shown in Fig. 6. The SEM micrographs of these biocomposite appear to be similar, however 10 wt% fibre filled composite clearly indicates the uniform distribution of the fibre in the PLA matrix with no fibre pool out. This is an indication of good interfacial adhesion between MFJ and PLA matrix. The increase in the tensile strength of 10 wt% of composites also supports this fact.

The interfacial interactions between MFJ and PLA matrix thus have an important effect on the effective transfer of the local stress. In case of other compositions, more fibre agglomeration as well as

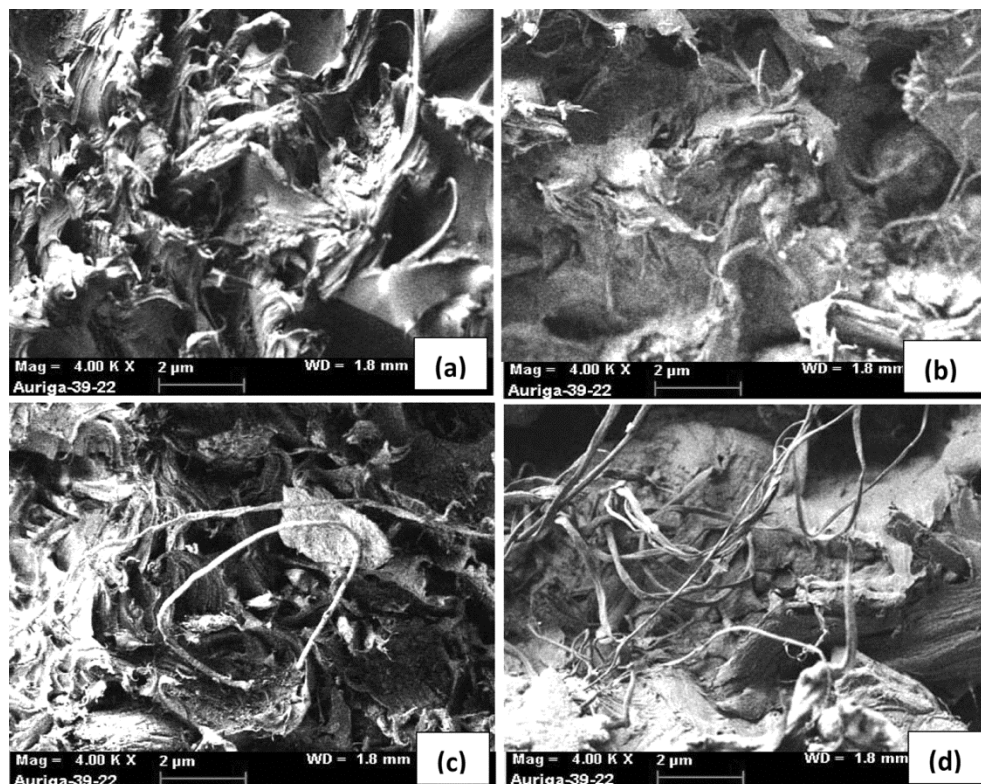


Fig. 6 — SEM image of MFJ/PLA composites (a) 0 wt% MFJ, (b) 10 wt% MFJ, (c) 20 wt% MFJ, and (d) 30 wt% MFJ fibres

pull out is observed which indicates the weak adhesion between the fibre and the matrix. However, the predication of interfacial adhesion based morphological analysis of lignocellulose/PLA composites is relatively complicated, and contradictory observations in many cases are reported in the literature²⁹. For example, on the basis of SEM analysis of PLA containing 40 wt % of jute fabric, Plackett *et al.*³⁰ have found voids around the fibres and concluded that adhesion must be improved, although they reported the increase in strength of this composite as compared to that of neat matrix and explained it with good adhesion.

3.6 FTIR Analysis

The chemical structures of neat PLA, MFJ and 10 wt% fibre loaded biocomposites are characterized by FTIR analysis (Fig. 7). The FTIR spectra of 10 wt% fibre loaded biocomposite show the characteristics of both PLA and MFJ fibre. Due to the absence of carbonyl group, MFJ fibre does not show the peak at around 1700–1760 cm^{-1} . The MFJ spectrum shows distinctive peaks and bands for carbohydrates, such as a broad band in the range of 3760–3010 cm^{-1} indicates hydrogen bonded hydroxyl groups, CH_2 stretching appears at 2932 cm^{-1} , while O–C stretching occurs in the range of 1180–960 cm^{-1} and anhydroglucose ring stretching vibrations can be seen in the range of 861–575 cm^{-1} .

After the composite fabrication, FTIR spectra of biocomposites demonstrate an additional intense peak at around 1747 cm^{-1} , this is arising from the stretching frequency of carbonyl group in ester of PLA. The relative intensity of the characteristic peak of MFJ decreases at around 3400 cm^{-1} for 10 wt% fibre loaded composite which is

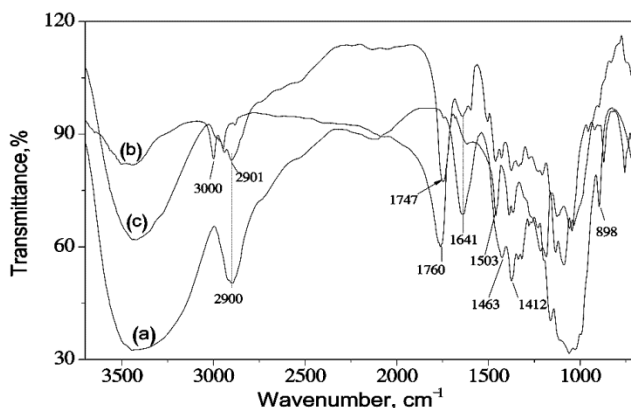


Fig. 7 — FTIR spectra of (a) MFJ, (b) neat PLA, and (c) 10 wt% MFJ/PLA biocomposite

responsible for hydrophilic –OH band stretching in cellulose. Additionally, peaks at around 3000 cm^{-1} have been observed, which belong to the asymmetric and symmetric stretching of CH_2 group of the PLA. This peak is absent in case of 10 wt% fibre loaded composite, probably due to the bond formation.

Figure 8 shows the WAXRD patterns of the crystalline structure of neat PLA, MFJ fibre and 10 wt% fibre loaded biocomposite. The MFJ fibre exhibits the characteristics peaks at $2\theta = 12.2^\circ$, 19.83° , and 21.83° which is attributed to the 110, 021 and 002 plane of cellulose II polymorph structure respectively³¹. In a case of PLA matrix, the scattering curves has four main characteristic peaks at 2θ of 12.73° , 16.62° , 18.88° and 22.17° which is assigned to the plane 010, 200, 203, and 015. The WAXRD curve of all composites shows the mixed characteristic of MFJ fibre and PLA. However, this effect is more pronounced in higher fibre loading percentage. The peaks at $2\theta = 16.62^\circ$ (200), and 22.55° (015) arises from PLA and the peak at around 19.27° (021) from MFJ fibres are observed. However, the peak positions and total number of peaks are not same to the components of biocomposite. A new plane 010 at $2\theta = 16.98^\circ$ demonstrates that MFJ fibre might be folded with PLA matrix which may result in increased crystallinity. The 10 wt% and 30 wt% fibre loaded biocomposite shows the mixed characteristics of MFJC and PLA. The peaks at $2\theta = 16.62^\circ$ (200), and 22.55° (015) come from PLA and peak at 19.27° (021) comes from MFJC.

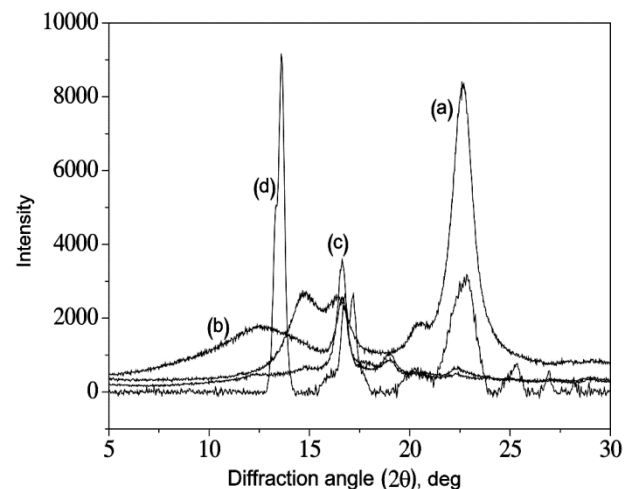


Fig. 8 — WAXRD diffractogram of (a) MFJ, (b) neat PLA, (c) 10 wt% MFJ/PLA, and (d) 30wt% MFJ/PLA biocomposites

4 Conclusion

The present study shows that the microfibrillated jute fibres could be used as “green” reinforcing filler in PLA and other polymers. It has been found that the fibre filled PLA shows considerable modifications of physical and mechanical properties compared to the neat PLA. The microfibrillated jute fibre reinforced PLA composites are found to be stiffer and stronger than the neat PLA. The reinforcement with 10 wt% fibre shows higher storage modulus and lower loss modulus. The morphological analysis of composites of 10 wt% microfibrillated jute fibre indicates more uniform dispersion of fibres than other compositions. This fact is supported by improvement in tensile strength and modulus. The WAXRD results also indicate the microstructure changes for these composites. However, thermal stability of biocomposites decreases proportionally with the addition of microfibrillated jute fibre. On the basis of this study, it is clear that fibre loading has an important effect on the composite properties, which can be further improved with loading of optimum amount, fibre size and shape, suitable compatibilizer and the work in this direction is continued.

Acknowledgement

The authors would like to extend their sincere appreciation to the Deanship of Scientific Research at King Saud University for funding support through the Research Group Project No. RGP-095. The authors also gratefully acknowledge the help by Chairman, Bangladesh Council of Scientific and Industrial Research, Dhaka, Bangladesh for composite testing.

References

- Sun Y H, San Y J & Nam K M, *Polym Degrad Stab*, 87 (2005) 131.
- Lee S H & Wang S, *Composites: Part A*, 37 (2006) 80.
- Mehta R, Kumar V, Bhunia H & Upadhyay S N, *J Macromol Sci Polym Rev*, 45 (2005) 325.
- Nagarajan S & Reddy B S R, *J Sci Ind Res*, 68 (2009) 993.
- Oksman K, Skrifvers M & Selin J F, *Compos Sci Technol*, 63 (2003) 1317.
- Shah D U, Schubel P J, Clifford M J & Licence P, *Polym Compos*, 33 (2012) 1494.
- Mathew A P, Oksman K & Sain M, *J Appl Polym Sci*, 97 (2005) 2014.
- Oksman K, Mathew A P, Badson D & Kvin I, *Compos Sci Technol*, 66 (2006) 2776.
- Lasseuguette E, *Cellulose*, 15 (2008), 571.
- Lin N, Chem G, Huang J, Dufresne A & Chang P R, *J Appl Polym Sci*, 113 (2009) 3417.
- Lonnberg H, Larsson K, Lindstrom T, Hult A & Malmstrom E, *ACS Appl Mater Interfaces*, 3 (2011) 1426.
- Quintana R, Olivier Persenaire O, Lemmouchi Y, Bonnaud L & Dubois P, *Euro Polym J*, 57 (2014) 30.
- Asaithambi B, Ganesan G & Anando Kumar, *Fiber Polym*, 15 (2014) 847.
- Avella M, Gaceva G B, Buzarovska A, Errico M E, Gentile G & Grozdanov A, *J Appl Polym Sci*, 108 (2008) 3542.
- Khan G M A, Terano M & Alam M S, *J Polym Mater*, 30 (2013) 397.
- Khan G M A, Shaheruzzaman M, Rahman M H, Razzaque S M A, Islam M S & Alam M S, *Fiber Polym*, 10 (2009) 65.
- Mondal M I H & Khan G M A, *Cell Chem Technol*, 42 (2008) 9.
- Tappi Test Methods, T 203 cm-09: Alpha-, Beta- and Gamma-Cellulose in Pulp*. (Tappi Press: Atlanta), 1999. <http://imisrise.tappi.org/TAPPI/Products/01/T/0104T203.aspx>.
- Khan G M A, Palash S R S, Alam M S, Chakraborty A K, Gafur M A & Terano M, *Polym Compos*, 33 (2012) 764.
- Kalam A, Berhan M N & Ismail H, *J Reinforced Plastics Compos*, 29 (2010) 3173.
- Wang S, Shanks R A & Hodzic A, *Macromol Mater Eng*, 289 (2004) 447.
- Jacob M, Francis B & Thomas S, *Polym Compos*, 27 (2006) 671.
- Petersen K, Nielsen P & Olsen B M, *Starch/Stark*, 53 (2001) 356.
- Rodrig H, Bash A & Lewin M, *J Polym Sci Part A: Polym Chem*, 13 (1975) 1921.
- Rana A K, Mitra B C & Banerjee A N, *J Appl Polym Sci*, 71 (1999) 531.
- Liu X, Dever M, Fair N & Benson R S, *J Environ Polym Degrad*, 5 (1997) 225.
- Fay J J, Murphy C J, Thomos A & Sperling L H, *Polym Eng Sci*, 31 (1991) 1731.
- Han S O, Son W K, Youk J H & Park W H, *J Appl Polym Sci*, 107 (2008) 1954.
- Gabor F, Gabor D, Balazs I, Karoly R, Janos M & Bela P, *J Appl Polym Sci*, (2014). doi: 10.1002/app.39902
- Plackett D, Logstrup Andersen T, Batsberg Pedersen W & Nielsen L, *Compos Sci Technol*, 63 (2003) 1287.
- Khan G M A, Haque M A, Terano M & Alam M S, *J Appl Polym Sci*, 131 (2014) 40139.